DIVEX | DIVERSIFICATION DE L'EXPLORATION MINÉRALE AU QUÉBEC

RAPPORT FINAL
2010

Sous projet SC37

A new pyrite thermometer based on inter-sector element partitioning

Par

Vincent J. van Hinsberg, Julia King, Ana Guerra Marin, James R. Clark, Anthony E. Williams-Jones

**McGill University, Montréal, Québec
Anthony.williams-jones@mcgill.ca

Soumis à l'administration de DIVEX
Juin 2010 – Québec

DIVEX, Dép. de géologie et de génie géologique, 1065 av. de la Médecine, Université Laval, Québec, Québec, G1V 0A6
Tél. : (418) 656-2131 p.4574; Fax : (418) 656-7339; Courriel : info@divex.ca; Site web : www.divex.ca

1. INTRODUCTION

Pyrite is a common mineral in the Earth's crust, ranging from an accessory phase in many metamorphic and igneous rocks to a dominant component of most sulfidic ore deposits. Pyrite is stable over a wide spectrum of physicochemical conditions and environmental settings, including deposition at the surface (e.g., pyrite stalactites in old mine workings, pyrite films in H2S-emitting volcanic springs), formation during sediment diagenesis, and precipitation in high-temperature vents on the ocean floor, in hydrothermal ore deposits, and during metamorphism (cf. Berner 1984; Bowles and Vaughan 2006; Craig 1993; Reed and Palandri 2006). Although most pyrite is near-stoichiometric, in detail pyrite compositions, especially with respect to trace elements, are highly variable and reflects this diversity of host environments. Compositions are controlled by an intimate interplay of physical conditions (e.g., P, T, pH, $fO2$) and the chemistry of specific environments of deposition. These compositions thus provide a record of the physical and chemical conditions of pyrite formation. Together with its relative abundance, this makes pyrite a potentially useful tool to elucidate the conditions of ore-forming environments where it is commonly difficult to establish the physicochemical conditions of mineralization. For example, fluid inclusion thermometry is the most commoly used method at present, but this is generally applied to inclusions in quartz or other silicate phases that are not necessarily co-genetic with the ore minerals.

Unfortunately, at present the use of pyrite analyses in evaluating ore deposits is limited by the multitude of variables that control compositions; this makes it difficult to correlate composition conclusively with the many parameters involved in pyrite formation. However, for growth zoned pyrite grains, a subset of parameters can generally be assumed to be constant, and parameter controls on compositional differences between growth zones can be inferred with considerable confidence. Nevertheless, it remains difficult to differentiate between compositional variations that can be linked to specific chemical environments and/or changing physical conditions. Even when such a correlation can be established, the compositional dependencies for a given parameter have not been calibrated previously and therefore cannot be utilized readily to derive quantitative data.

In order to refine our understanding of the trace element variations between sectors within individual growth zones in pyrite, we have characterized natural pyrites and attempted to synthesize sector-zoned pyrites under varying physical conditions to calibrate compositional dependencies. Sector zoning develops when specific growth surfaces of a mineral preferentially take up or exclude elements. This results in compositionally distinct domains within a single, coeval growth zone, wherein the selective element distribution is controlled by differences in the morphology and charge of crystal growth surfaces; these surfaces represent different slices through otherwise homogenous crystal structures. With higher temperatures, the vibrational energy of crystallographic sites increases, and this limits the element segregation that can be attained at growth surfaces. Consequently, there is a decrease in inter-sector element partitioning with increasing temperature, and this forms the basis of its use as a thermometer (van Hinsberg et al. 2006). Because the host chemistry is identical for the different growth surfaces at all times, sector zoning is entirely independent of the local environment. Therefore, despite variations in the absolute concentrations of elements in the host fluid, the relative compositional differences between sectors will be unaffected, which makes sector zoning a potentially robust thermometer that can be applied directly to settings outside its calibrated environment.

2. SECTOR ZONING

Compositional zoning in minerals generally reflects changes in the physical or chemical conditions of the growth environment, e.g., changes in temperature or variations in fluid composition. Compositional sector zoning, on the other hand, develops at static chemical and physical conditions due to differences in the element uptake at different growth surfaces of the mineral. This type of zoning is common in many different minerals and geological settings, including clinopyroxene and feldspar in magmatic rocks (Bryan 1974; Lofgren et al. 2006), staurolite, tourmaline and andalusite in metamorphic rocks (Watson 1996 and references therein; van Hinsberg et al. 2006), calcite and tourmaline in sedimentary deposits (Dickson 1991; Henry et al. 1999), and quartz, pyrite and arsenopyrite in hydrothermal deposits (Onasch and Vennemann 1995; Vesselinov and Kerestedjian 1995; Zacharias et al. 2004; Chouinard et al. 2005; Pacevski et al. 2008). Compositional variations between zones occur for major and trace elements (Bryan 1974; Chouinard et al. 2005; Lofgren et al. 2006; van Hinsberg et al. 2006) as well as for isotopic signatures ($\delta^{13}C$ and $\delta^{18}O$ in calcite - Dickson 1991; $\delta^{18}O$ in quartz – Onasch and Vennemann 1995; $\delta^{11}B$ in tourmaline - van Hinsberg and Marschall 2007).

These chemical and isotopic differences are often very distinct and may exceed those observed in associated normal growth zoning.

For sector zoning to develop, a mineral grain must grow on a number of growth surfaces that are crystallographically distinct (i.e., not equivalent through symmetry operators). Secondly, these various growth surfaces must be dissimilar in surface properties in order to vary in terms of element uptake. Surface morphology and charge have previously been recognized as important variables that can induce compositional sector variations (Hollister 1970; Watson and Liang 1995; Watson 1996; van Hinsberg et al. 2006). Aside from a primary element preference in response to morphological factors and element charge, sector zoning is commonly associated with a secondary preferential uptake to balance the primary uptake (e.g., preferential uptake of Mg^{2+} over Al^{3+} following Ca^{2+} incorporation on the Na^{+} site of tourmaline - van Hinsberg and Marschall 2007).

Sector zoning can develop during both equilibrium and disequilibrium mineral growth (Watson and Liang 1995; Watson 1996; van Hinsberg and Schumacher 2007; Lofgren et al. 2006, Shtukenberg et al. 2009). For disequilibrium, differences in surface growth rates can lead to exhaustion of the local growth environment in compatible elements, as well as a build up of incompatible elements for fast growing surfaces. This in turn may result in sector compositions that are not in equilibrium with the host bulk composition. Differences in element diffusivity towards or away from this boundary growth zone will augment this effect. For conditions of thermodynamic equilibrium between mineral and host environment, the various growth surfaces must be in chemical equilibrium, both with each other and with the host. However, given that the thermodynamic properties of the host environment are uniform, the different surfaces can only reach equilibrium by establishing compositions that for each surface are in thermodynamic equilibrium. It is also noteworthy that crystallographic surface differences that lead to differential element uptakes at variable growth rates do not persist in the bulk mineral, and therefore sectors are in disequilibrium when no longer on the actual growth surface. This leads to diffusional re-equilibration of compositional contrasts over time and sector zoning is thus a time-dependent feature.

In the case of equilibrium sector zoning, the chemical environment is identical for the various growth surfaces, and inter-sector element distributions are a measure of crystallographic differences that are sensitive only to variations in the physical conditions. For example, increasing temperature will result in elaxation of the crystal lattice, which will reduce the element selectivity of the various growth surfaces, and hence decrease compositional contrasts between sectors. Such temperature dependent inter-sector element partitioning has been calibrated by van Hinsberg and Schumacher (2007) for tourmaline.

Sector zoning also provides information on the element exchange vectors that operate in a mineral, because the compositional differences between sectors are controlled entirely by crystallography. In the case of pyrite, this allowed Chouinard et al. (2005) to determine the incorporation mechanism for Au.

3. METHODS

3.1. Natural Samples

In this study we investigated natural pyrite grains from two gold deposits; the Canadian Malartic deposit in Quebec, and the Bawone and Binebase high-sulphidation deposits on the island of Sangihe in Indonesia. Pyrite in the Canadian Malartic deposit is hosted by greenschist-facies greywackes and porphyries of Archaean age. Pyrite occurs predominantly as disseminated grains associated with hydrothermal quartz-carbonate veins and biotitic and Kfeldspathic alteration haloes, and in lesser abundance in the overprinting metamorphic assemblage (bt + pl + q ± chl ± ep ± ms ± Kf). Sector zoning has only been observed in the former. Pyrite in the Bawone and Binebase deposits occurs mainly as disseminated grains, colloform masses and cross-cutting veins. At Bawone and Binebase, sector zoning has been observed in all pyrite types, but is most common in colloform pyrite, in association with alunite, barite and enargite.

Polished thin sections of drill core samples were imaged and quantitatively analysed on a JEOL-8900L electron microprobe. Back-scattered electron imaging was used to locate regions with sector zoning, which were subsequently X-ray mapped for Cu, S, As and Fe. Quantitative spot analyses for Fe, S, As, Cu, Ni, Se and Te were conducted in WDS mode, using a 20 kV acceleration voltage, 50 nA beam current, and a focused beam. Peak and background count times and standards were; Fe (pyrite, 20s), As (arsenopyrite, 115s), S (pyrite, 20s), Ni (CoNiAs, 115s), Se (AgBiSe2, 115s), Te (CdTe, 100s) and Cu (chalcopyrite, 100s). Detection limits for the trace elements were below 100 ppm.

Sector zoning in pyrite is not always obvious even in back-scattered electron imaging and it can be difficult to pinpoint exact sector boundaries. We therefore developed the following approach to quantify the inter-sector element partitioning in pyrite. Grains were initially mapped at low magnification to pinpoint regions of sector zoning, and these regions were subsequently mapped at high resolution. We then used these maps to position two corresponding line-scans, perpendicular to the growth zones, but within the two respective sectors. Maps and line-scans were referenced to each other and the two line-scans matched based on growth zoning in the X-ray maps. Finally, the matched line-scans were normalized to produce equivalent points from which the element partitioning was determined.

3.2. Experiments

In the experimental part of this project we hydrothermally synthesized pyrite at varying conditions of pressure, temperature, *f*O2 and pH. Four different experimental approaches were investigated (Fig. 1). In the first approach, a fragment of marcasite was suspended from a pure Fe wire in a steel autoclave above a 10 wt% $FeCl_2$ solution doped with ~100 ppm As, Se, Cu, Sb and Te. The autoclave was subsequently externally heated for 3 weeks to 300°C with temperature controlled to within 2°C, and the degree of fill ensured a vapour-saturated pressure. A 2 x 2 mm cubic pyrite seed crystal was also added to the solution. At the experimental temperature, the marcasite was submerged in the solution, and should convert to stable pyrite, either directly, or by dissolution and re-precipitation on the seed and autoclave walls. The presence of native iron, pyrite and Fe-oxide on the walls of the autoclave, buffered *f*S2 and *f*O2 during the experiment.

In the second approach, we employed a thermal gradient technique where one end of the autoclave was positioned in a tube furnace and heated to 270°C and the opposite end cooled by a constant flow of compressed air. The temperature at the cool end was monitored using a thermocouple inserted into the autoclave. The steel autoclave was filled with the same starting solution and a small pyrite seed crystal at the cooler end. At the heated end, a large fragment of Sangihe pyrite was placed on top of a quartz-glass tube to avoid it moving from the hot zone. A temperature gradient of approximately 70°C was obtained at vapour-saturated pressure, and maintained for three weeks. In this approach, pyrite should dissolve at the hot end and re-precipitate at the cooler end of the autoclave.

In the final two approaches TiO_2-coated Ti-autoclaves were filled with a 25 wt% $FeCl_2$ solution containing ~100 ppm each of As, Se, Cu, Sb and Te, and a small pyrite seed crystal. In the third set of experiments, a small quartz-glass tube with Al_2S_3 was added; the Al_2S_3 reacts with water vapour at run conditions to release H_2S, which in turn should react with the solution to precipitate pyrite. Autoclaves were externally heated at 200°C and 350°C at vapour-saturated pressure for 4 weeks and quenched in water (temperature controlled to within 2°C). In the final set of experiments, natural native sulphur powder was used instead of the Al_2S_3 tube, with the similar aim of reacting with the solution which should lead to pyrite precipitation. Experiments were run at 200°C and 350°C for three weeks at vapour-saturated pressure (temperature controlled to within 2°C).

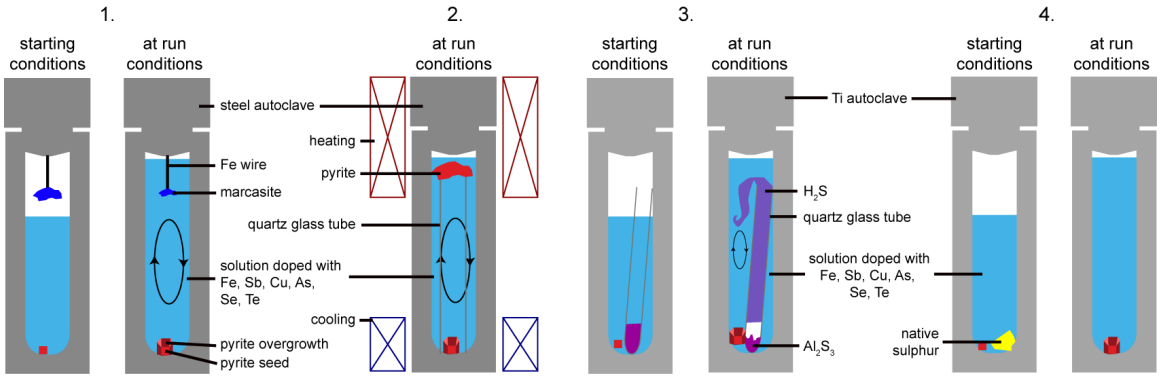

Figure 1. Experimental approaches used in hydrothermal syntheses of pyrite. Approach 1 centers on the replacement of marcasite by pyrite; 2 on the dissolution and re-precipitation of pyrite in a thermal gradient; in 3, H_2S is produced by reaction of Al_2S_3 with water leading to pyrite precipitation; and in 4, pyrite precipitation is brought about by reaction of solution with native sulphur.

4. RESULTS

Three main types of sector zoning were observed in the natural pyrites: cross-shaped sector zoning, wedge-shaped sector zoning (most common in colloform pyrite), and trigonal sector zoning (Fig 2). All three types occur in Sangihe pyrite, whereas Malartic pyrite exhibits only rare examples of the cross-shaped type.

Results indicate that Cu, Se, As and Te show inter-sector partitioning that is significant and systematic. Copper is the predominant element in Sanighe sector zoned pyrite, with concentrations varying by a factor of 4 between high-Cu sectors (lighter grey areas in BSE images and X-ray maps; see Fig. 2) and low-Cu dark sectors. The distribution of As is similar to that of Cu, whereas that of Se shows opposite behavior. Nickel also exhibits variations that are sector zoned, but concentrations in low Cu sectors are generally below the detection limits and therefore cannot be quantitatively evaluated. Variations in Cu between sectors and growth horizons are balanced by corresponding variations in Fe.

Systematic changes in inter-sector partition coefficients of Cu are observed for transects perpendicular to the growth zoning, and such changes are reproducible through different areas of colloform pyrite bands.

Synthesis experiments were largely unsuccessful. Pyrite formed in the thermal gradient approach, but grains were too small to characterize. In the marcasite-bearing experiments, marcasite grew at the expense of pyrite and no stable assemblage had developed at the end of the run. The experiments with H_2S did not produce any precipitates, and in fact resulted in complete dissolution of the pyrite seed crystals. The addition of additional $FeCl_2$ to these latter experiments did not change the results. The final set of experiments produced a stable assemblage of native sulphur and Fe-(hydr)oxide, rather than pyrite. At 350^{o}C, native sulphur was present as rounded globules indicating that it was liquid during the experiment, whereas it was present as angular fragments in the 200^{o}C run product.

5. DISCUSSION

5.1. Equilibrium

In order to assess the potential of inter-sector element partitioning in pyrite as a record of the physical conditions of formation, it is imperative to establish whether the sector zoning developed due to kinetic effects, or whether it reflects equilibrium surface partitioning. Following the approach of van Hinsberg et al. (2006), we checked for correlations between differences in growth rate and inter-sector element partitioning. For the colloform pyrites in particular, the differences in growth rates between sectors are very small and do not vary significantly from core to rim. However, inter-sector partition coefficients vary strongly, suggesting that partitioning is not controlled by differences in growth rates. Indeed, for the pyrite studied in this project, we find that there is no correlation between changes in sector boundary angles and inter-sector element partitioning in the pyrites.

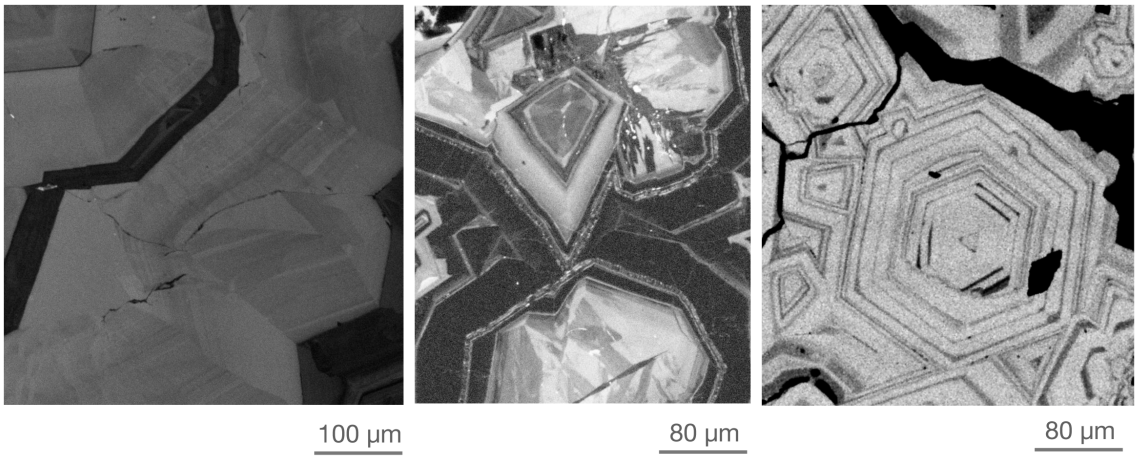

Figure 2. Types of sector zoning shown by Cu X-ray maps of Sangihe pyrite: left – wedge-shaped sectors in colloform pyrite; center – cross-shaped sector zoning; right – trigonal sector zoning.

Sector zones also display highly consistent differences across multiple sector boundaries along given growth horizons despite variations in growth band thicknesses (e.g., colloform pyrite in Fig. 2a). This consistency combined with the lack of correlation with growth rate variations suggest that there was only a minor contribution from kinetic factors. Therefore, we conclude that inter-sector differences for pyrite reflect equilibrium partitioning at growth surfaces, and that inter-sector partitioning should be suitable to provide a means of quantifying physical conditions during growth.

5.2. Surface structure

The compositional trace of growth horizons in pyrite grains allows us to evaluate the controlling surfaces that operated during crystal growth. The dominant growth surfaces in these pyrites are |110| and |111| (Fig. 3), which is consistent with the conslusions of Chouinard et al. (2005). The colloform pyrite additionally displays [113] surfaces (and possibly others), although these may be due to sectioning effects.

A crystallographic model for the |110|, |111| and |113| surfaces (Fig. 4) shows that they vary in both surface morphology and anion density. Both factors have been implicated in the development of sector zoning, and both affect the attraction of elements to the mineral surface, the strength of subsequent bonding, and thus lead to differential element uptake (Hollister 1970; Watson 1996; van Hinsberg et al. 2006). Unfortunately, the valence of Cu in the pyrite studied here is unknown, which prohibits us from evaluating whether anion density or morphology plays the dominant role in its preferential uptake on |110| surfaces.

5.3. Inter-sector element partitioning

Analytical transects from core to rim through growth-zoned pyrite in Sangihe samples show large variations in Cu concentrations. However, patterns for the different sectors are consistent and are characterized by systematic offsets in composition (Fig. 5a). The Cu inter-sector partition coefficients calculated from the differences in Cu concentrations between sectors also have strong and systematic variations, but these are notably decoupled from the Cu variations (Fig. 5b). Partitioning shows an initial increase, a subsequent decrease to values close to unity, and finally a rapid increase to high D-values.

As noted above, variations in inter-sector element partitioning can only be caused by variations in the physico-chemical properties of the environment of formation. Temperature is the most likely physical factor to affect crystal structures and hence the preferential uptake of elements, with decreasing partitioning expected with increasing temperature (cf. van Hinsberg and Schumacher 2007). The partitioning observed in Fig. 5b indicates an initial decrease in temperature, followed by an increase to temperatures where sector zoning has almost disappeared, and finally growth at rapidly decreasing temperature. In contrast to the partition coefficients, variations in actual Cu concentrations are markedly decoupled from the inter-sector partitioning, which suggests that Cu concentrations were not controlled by temperature, but rather by changes in the chemical environment. This decoupling is especially clear for the kink in Cu concentration near the rim, whereas

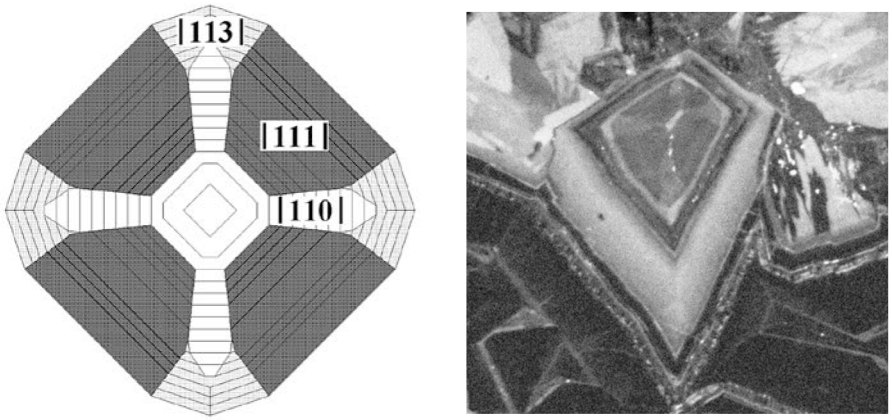

Figure 3. Left - cross-section through a pyrite grain with |110|-|111|-|113| sector zoning (from Chouinard et al. 2005); right - Cu X-ray map for cross-shaped sector zoning in a Sangihe pyrite grain (see Fig. 2 for scale).

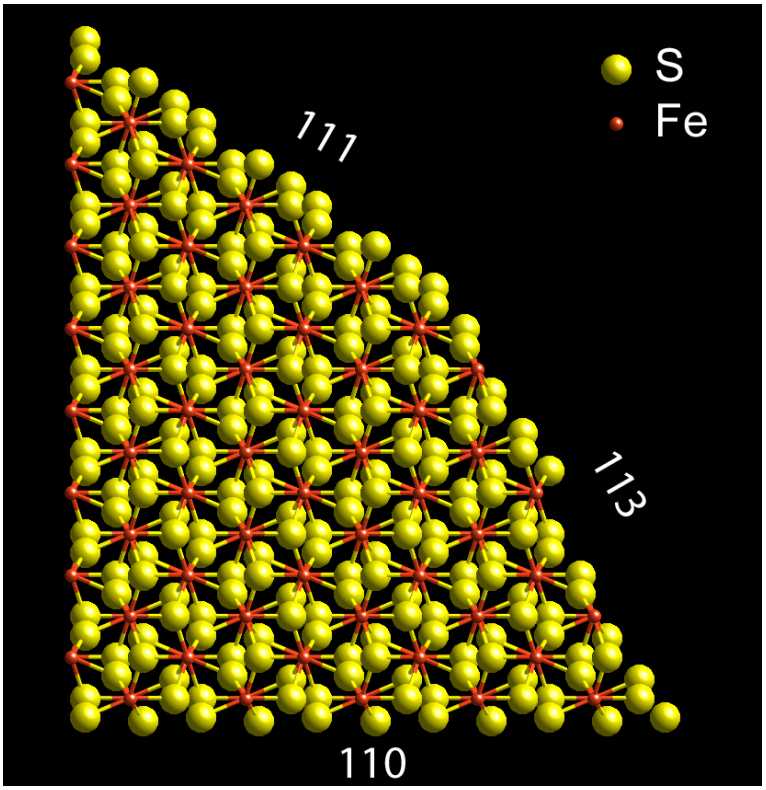

Figure 4. Crystallographic section through pyrite showing the 110, 111 and 113 surfaces.

the partition coefficients continue to increase (with decreasing temperature; Fig. 5).

6. CONCLUSIONS AND FUTURE DIRECTIONS

Sector zoning in pyrite, formed by differential uptake of elements on different growth surfaces, leads to systematic inter-sector partitioning. Although these compositional differences are independent of the

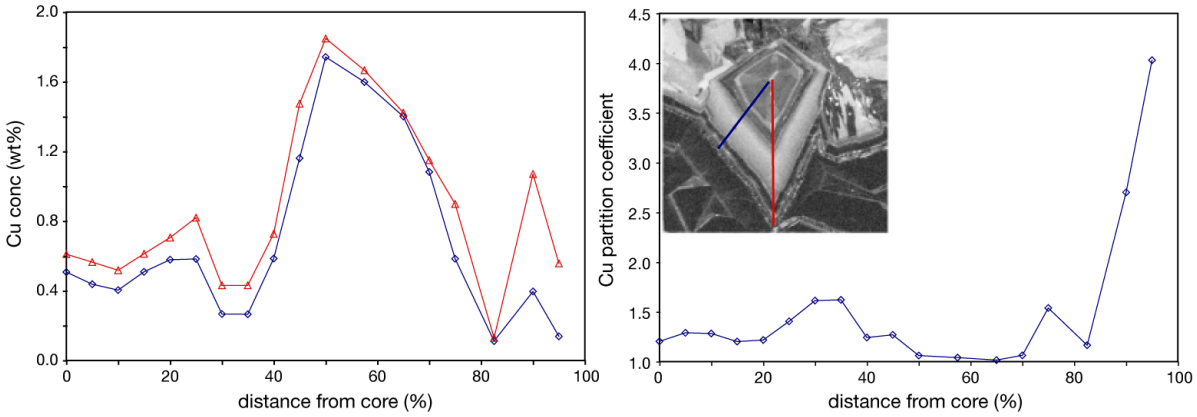

Figure 5. Left - normalized transects of Cu concentrations for equivalent points in the |110| and |111| sectors of a Sangihe pyrite; right - corresponding inter-sector Cu partition coefficients. Transect positions are shown on the inset map.

chemistry of the growth environment, inter-sector partitioning coefficients only reflect the physical conditions present at the time of formation. We propose that variations in partition coefficients in pyrite are mainly a product of temperature, which allows changes in these coefficients to be used as monitors of temperature history.

The independence of variations in element partitioning to the chemical environment makes sector zoning a perfect monitor of physical conditions, and consequently allows the chemical variations between growth zones to be evaluated independently. These factors together with the ubiquity of pyrite in crustal rocks in general and hydrothermal alteration zones in particular make pyrite a potentially powerful tool to elucidate the chemical and physical conditions of depositional environments, which will be especially valuable in evaluating the conditions of ore formation.

In future work, we plan to calibrate the temperature dependence of inter-sector element partitioning, using a dual approach of further thermal gradient synthesis experiments and investigation of natural sector-zoned pyrites from well-constrained localities in terms of pressure and temperature.

7. ACKNOWLEDGEMENTS

We thank Divex for funding, Osisko Mining Corp. and East Asia Minerals Corp. for access to samples of the Canadian Malartic and Sangihe gold deposits, respectively.

8. REFERENCES

Berner, R.A. (1984), Sedimentary pyrite formation: An update, Geochimica et Cosmochimica Acta 48, 605-615.

Bowles, J.F.W., Vaughan, D.J. (in press) Oxides and Sulphides. Vol. 5A. Rock-Forming Minerals (Deer, Howie, Zussman), Geological Society of London Publication.

Bryan, W.B. (1974) Fe-Mg relationships in sector-zoned submarine basalt plagioclase. Earth and Planetary Science Letters 24, 157-165.

Chouinard, A., Paquette, J., Williams-Jones, A.E. (2005) Crystallographic controls on trace-element incorporation in auriferous pyrite from the Pascua epithermal high-sulphidation deposit, Chili-Argentina. Canadian Mineralogist 43, 951-963.

Craig, J.R. (1993) The metamorphism of pyrite and pyritic ores: an overview. Mineralogical Magazine 57, 3-18.

Dickson, J.A.D. (1991) Disequilibrium carbon and oxygen isotope variations in natural calcite. Nature 353, 842-844.

Henry, D.J., Kirkland, B.L., Kirkland, D.W. (1999) Sector-zoned tourmaline from the cap rock of a salt dome. European Journal of Mineralogy 11, 263-280.

Hollister, S. (1970) Origin, mechanism and consequences of compositional sector zoning in staurolite. American Mineralogist 55, 742-766.

Krinov, D.I. (2008) Geochemical zoning of pyrite and arsenopyrite Individuals from the Klyuchevskoe Gold Deposit, Eastern Transbaikalia. Geochemistry International 46, 1005-1015.

Lofgren, G.E., Huss, G.R., Wasserburg, G.J. (2006) An experimental study of trace-element partitioning between Ti-Al-clinopyroxene and melt: Equilibrium and kinetic effects including sector zoning. American Mineralogist 91, 1596-1606.

Onasch, C.M., Vennemann, T.W. (1995) Disequilibrium partitioning of oxygen isotopes associated with sector zoning in quartz. Geology 23, 1103-1106.

Pacevski, A., Libowitzky, E., Zivkovic, P., Dimitrijevic, R., Cvetkovic, L. (2008) Copper-bearing pyrite from the Coka Marin polymetallic deposit, Serbia: Mineral inclusions or true solid-solution? The Canadian Mineralogist 46, 249-261.

Reed, M.H., Palandri, J. (2006) Sulfide Mineral Precipitation from Hydrothermal Fluids. Reviews in Mineralogy and Geochemistry 61, 609-631.

Shtukenberg, A.G., Punin, Yu., O., Artamonova, O.I. (2009) Effect of crystal composition and growth rate on sector zoning in solid solutions grown from aqueous solutions. Mineralogical Magazine 73, 385-398.

van Hinsberg, V.J., Schumacher, J.C., Kearns, S., Mason, P.R.D., Franz, G. (2006) Hourglass sector zoning in metamorphic tourmaline and resultant major and trace-element fractionation. American Mineralogist 91, 717-728.

van Hinsberg, V.J., Marschall, H.R. (2007) Boron isotope and light element sector zoning in tourmaline: Implications for the formation of B-isotopic signatures. Chemical Geology 238, 141-148.

van Hinsberg, V.J. & Schumacher, J.C. (2007) Intersector element partitioning in tourmaline: a potentially powerful single crystal thermometer.

Contributions to Mineralogy and Petrology 153, 289-301.

Vesselinov, I., Kerestedjian, T. (1995) Kinetic aspects of sector zoning in arsenopyrite: a case study. Mineralogy and Petrology 52, 85-106.

Watson, E.B., Liang, Y. (1995) A simple model for sector zoning in slowly grown crystals: Implications for growth rate and lattice diffusion, with emphasis on accessory minerals in crustal rocks. American Mineralogist 80, 1179-1187

Watson, E.B. (1996) Surface enrichment and trace-element uptake during crystal growth. Geochimica et Cosmochimica Acta 60, 5013-5020.

Zacharias, J, Fryda, J, Paterova, B, Mihaljevic, M (2004) Arsenopyrite and As-bearing pyrite from the Roudny deposit, Bohemian Massif. Mineralogical Magazine 68, 31-46.